

九州工業大学学術機関リポジトリ



Title	Electronic structure and electrical properties of amorphous OsO ₂
Author(s)	Hayakawa, Yuko; Kohiki, Shigemi; Arai, Masao; Yoshikawa, Hideki; Fukushima, Sei; Wagatsuma, Kazuaki; Oku, Masaoki; Shoji, Fumiya
Issue Date	1999-05
URL	http://hdl.handle.net/10228/649
Rights	Copyright © 1999 American Physical Society

Electronic structure and electrical properties of amorphous OsO₂

Yuko Hayakawa and Shigemi Kohiki

Department of Materials Science, Kyusyu Institute of Technology, Kita-kyusyu 804-8550, Japan

Masao Arai, Hideki Yoshikawa, and Sei Fukushima

National Institute for Research in Inorganic Materials, Tsukuba, Ibaraki 305-0044, Japan

Kazuaki Wagatsuma and Masaoki Oku

Institute for Materials Research, Tohoku University, Sendai 980-8577, Japan

Fumiya Shoji

Department of Electrical Engineering, Kyushu Kyoritsu University, Kita-kyusyu 807-8585, Japan

(Received 9 September 1998; revised manuscript received 18 November 1998)

The valence-band spectrum of an amorphous OsO₂ film deposited by glow discharge of OsO₄ vapor can be predicted well with calculated electronic band structure of crystalline OsO₂ from first principles using the liner-muffin-tin-orbital method with the local-density approximation. Resistivity of the amorphous OsO₂ was less than $6 \times 10^{-3} \Omega \text{ cm}$ at 80 K, and it was almost temperature independent, but the temperature coefficient of resistivity was negative. The Hall coefficient of the amorphous OsO₂ increased with temperature, and was saturated at around 220 K. Temperature dependence of the Hall mobility was proportional to $T^{3/2}$, and it implies that the scattering of charged carriers by ionized atoms is dominant below 220 K.

[S0163-1829(99)04817-1]

Rutile-type oxides of transition metals show a variety of electrical properties such as insulating (TiO₂), metallic (RuO₂), and semiconducting (NbO₂).¹ RuO₂ has been widely used as an oxide electrode in microelectronics fabrications. Reported resistivities for single crystals of RuO₂ and OsO₂ are 5×10^{-5} and $6 \times 10^{-5} \Omega \text{ cm}$ at room temperature, respectively.¹ Similar temperature dependence of the resistivity, increasing with increasing the temperature, has also been reported.¹

Electronic structure and electrical properties of OsO₂ thin films are of interest in relation to the development of conducting electrodes because the films even in the amorphous state can avoid sufficiently charging effects in high-magnification transmission and secondary electron microscopies, and electron spectroscopies.^{2,3} In this report we present a comparison of experimental and theoretical electronic structures, and results of electrical resistivity and Hall coefficient measurements on the amorphous OsO₂ film.

Amorphous OsO₂ films used in this study were deposited by dc glow discharge of OsO₄ vapor on single crystalline α -Al₂O₃ substrates at room temperature. Vapor of OsO₄ was introduced into deposition chamber evacuated to 1×10^{-3} Torr and the pressure was kept at 5×10^{-2} Torr during the deposition. The deposition rate was 300 nm/min when the applied voltage and current were 1.2 kV and 2 mA, respectively. Films of 1000 nm thickness were used in this experiment.

All the films deposited by dc glow discharge of OsO₄ vapor were amorphous. They showed no peaks except those from the α -Al₂O₃ substrate in the x-ray diffraction measurement.³ As shown in Fig. 1 no intensity drops due to shadowing effects were observed in the intensity curve with varying the impact angle α (α is measured from the surface) at a impact-collision ion scattering spectroscopy mode using the Li⁺ ion.⁴ A small difference (0.016 nm) in the nearest-

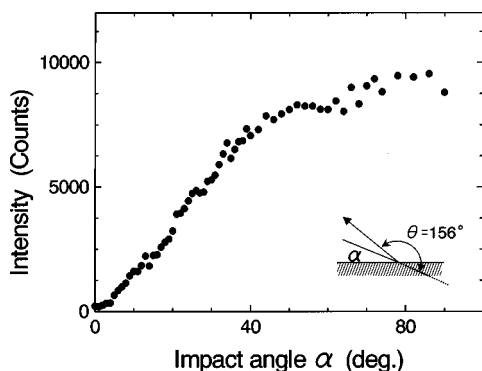


FIG. 1. Scattered Li⁺ ion intensity from the film with varying the impact angle α .

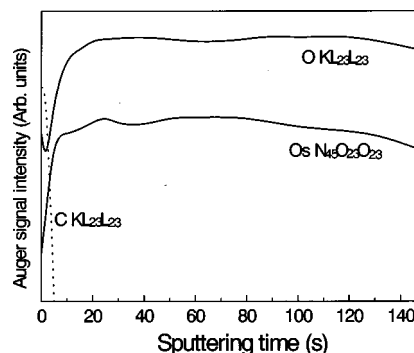


FIG. 2. Auger depth profile of the film. After the 1-keV Ar⁺ sputtering of 145 s, the sample suddenly showed a large charge-up effect due to disappearance of the conductive over-layer.

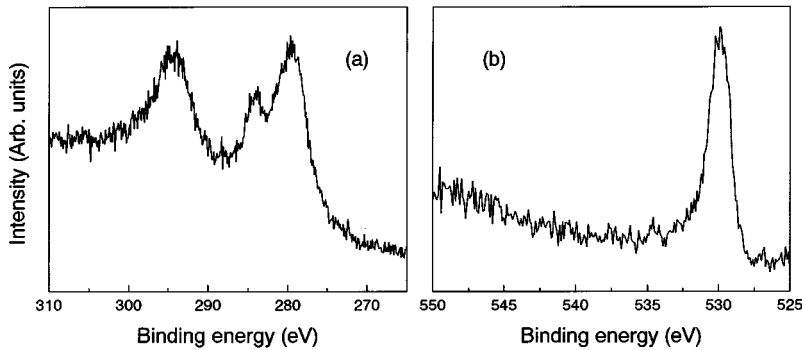


FIG. 3. Os $4d$ (a) and O $1s$ (b) spectra of the film.

neighbor distance for Os atoms between the experimental (for the amorphous OsO_2) and reported (for crystalline OsO_2) values, and larger coordination number for the amorphous OsO_2 ($N=5.8$) than for OsO_2 single crystal ($N=4$) were observed in the Os L_3 edge extended x-ray-absorption fine-structure measurements.⁵ As shown in Fig. 2, Auger electron spectroscopy with Ar^+ ion sputtering revealed that atoms of Os and O coexisted and homogeneously distributed in the amorphous films. No charge shift in the Auger electron kinetic energy was observed for the films.

In this experiment a hemispherical electron spectrometer calibrated by the Au $4f_{7/2}$ (83.79 eV) was used with monochromatized Al $K\alpha$ source, and the full width at half maximum of the Au $4f_{7/2}$ peak was 1.03 eV. The base pressure in the spectrometer was better than 5×10^{-10} Torr. The samples were repeatedly cleaned in acetone and methanol with ultrasonic vibration, and then transferred into the preparation chamber of the spectrometer. No charge correction was accomplished since the films were highly conductive and no charge shift was observed in the experiment. The statistical error amounted to ± 0.1 eV.

The Os $4d$ and O $1s$ spectra of the amorphous Os-O films are shown in Figs. 3(a) and 3(b). The observed Os $4d_{5/2}$ binding energy was 279.7 eV, which agreed well with that of OsO_2 (279.8 eV).⁶ Both the O $1s$ spectrum having a rather narrow single peak shape and the small C $1s$ peak between the Os $4d$ spin doublet suggest that a small peak of adventitious carbon consisted of C-C and C-H bonds and it scarcely altered the chemical state of the film. The experimental valence band spectrum of the amorphous OsO_2 film shown in Fig. 4 (lower panel) agreed well with the calculated density of states (DOS) of crystalline OsO_2 shown in Fig. 4 (upper panel).

We calculated the DOS of crystalline OsO_2 using the linear-muffin-tin-orbital method⁷ with the local-density approximation.⁸ The atomic positions used in this calculation of OsO_2 band structure are given in Ref. 9. The space group of OsO_2 is $P4_2/mnm$ and the measured values of the lattice parameters a and c are 0.4503 and 0.3184 nm, respectively. Two Os atoms are located at the positions $[0, 0, 0]$ and $[1/2, 1/2, 1/2]$ in lattice coordinates, and four O atoms are located at $[u, u, 0]$, $[1/2+u, 1/2-u, 1/2]$, $[1-u, 1-u, 0]$, and $[1/2-u, 1/2+u, 1/2]$ with a dimensionless internal coordinate $u=0.305$.

The resulting DOS of OsO_2 , shown in the upper panel of Fig. 4, qualitatively agrees with the previous calculation.¹⁰ The Fermi level is located at the dip of the DOS in the Os d bands. The O p bands appear separately at lower energy. The

p - d energy separation is 1–2 eV smaller than that of the previous calculation which was not self-consistent. The experimental bandwidth and spectral features at around 1, 5, and 7 eV of the amorphous OsO_2 correspond to those of the theoretical DOS of crystalline OsO_2 . The photoionization cross sections of the O $2p$ and Os $5d$ states by Al $K\alpha$ x rays are 0.24×10^{-3} and 0.12×10^{-1} Mb, respectively.¹¹ Since the DOS from 3 to 9 eV are dominated by the O $2p$ states as shown in Fig. 4 upper panel (thin dotted line), the observed intensity becomes smaller relative to that at around 1 eV dominated by the Os $5d$ states represented by a thin solid line in Fig. 4 upper panel.

The dc current and voltage contacts were made through gold lands evaporated in a four-point probe configuration on the film. Figure 5 shows the temperature dependence of the

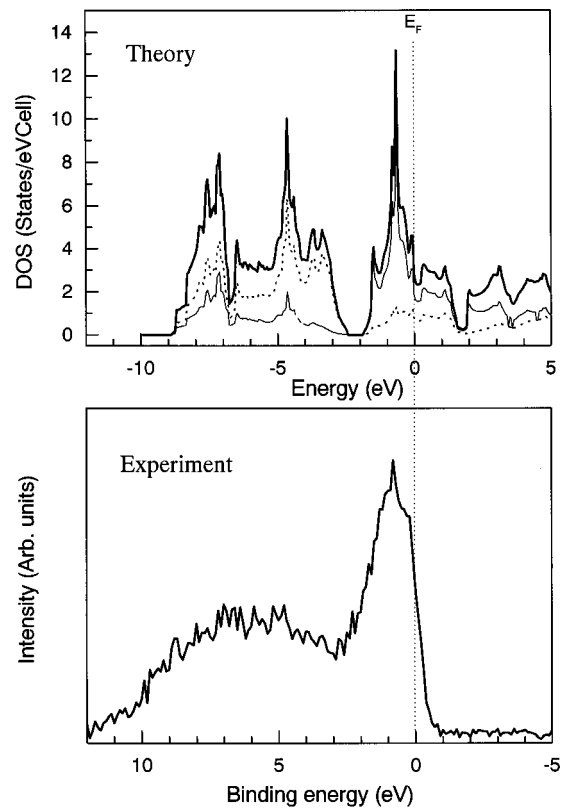


FIG. 4. Valence-band spectrum of the film (lower panel) and theoretical density of states (DOS) of crystalline OsO_2 (upper panel). Total DOS, O p partial DOS for two atoms, and Os d partial DOS for an atom are represented by the lines of bold solid, thin dotted, and thin solid, respectively.

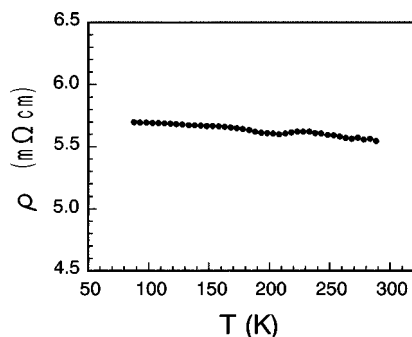


FIG. 5. Temperature dependence of resistivity of the film.

resistivity. The resistivity ρ of the amorphous OsO_2 is about $5.7 \times 10^{-3} \Omega \text{ cm}$ at 70 K and $5.6 \times 10^{-3} \Omega \text{ cm}$ at 300 K. The resistivity is larger than that of crystalline OsO_2 ($3 \times 10^{-6} \Omega \text{ cm}$ at 80 K and $6 \times 10^{-5} \Omega \text{ cm}$ at 300 K) (Ref. 1) by the order of two to three. The temperature dependence of the amorphous OsO_2 is also different from that of the crystalline OsO_2 . While the crystalline OsO_2 is metallic and the resistivity decreases as the temperature lowers, that of the amorphous OsO_2 is almost constant and slightly increases as the temperature lowers. It means that the temperature coefficient of resistivity (TCR) is negative for the amorphous OsO_2 . Such large resistivity and negative TCR are commonly observed for amorphous systems^{12,13} and resulted from the lack of long-range order in the amorphous OsO_2 .

The Hall effect of the film was measured by the van der Pauw method.¹⁴ As shown in Fig. 6, the Hall coefficient R_H of the amorphous OsO_2 increased rapidly with increasing the temperature and was saturated at around 220 K. The sign of the Hall coefficient must change from a positive to negative one below 120 K. From Figs. 5 and 6, it is readily understood that the Hall mobility given by $\mu_h = R_H/\rho$ increases with temperature below 220 K. As shown in the inset of Fig. 6, the temperature dependence of the Hall mobility, which

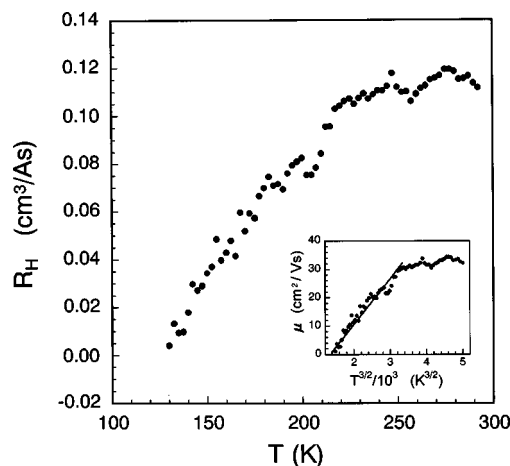


FIG. 6. Temperature dependence of Hall coefficient of the film. Inset: temperature dependence of Hall mobility. The straight line is a guide for eyes.

can be expressed as $\mu_h = cT^{3/2}$ where c is a constant, implies that the scattering of charged carriers by ionized atoms is dominant below 220 K.

We have presented the experimental results on the electronic band structure and electrical properties of the amorphous OsO_2 film. A first-principles band calculation of crystalline OsO_2 predicted well the valence band spectrum of the amorphous OsO_2 . The transport properties of the amorphous OsO_2 , largely different from those of crystalline OsO_2 , should reflect the random potentials due to the lack of long-range ordering in amorphous materials.

We would like to thank to O. K. Andersen and O. Jepsen for providing us the TB-LMTO-46 program, and Y. Shibata of Unitika Research Laboratories for support in this work. A part of this work was performed at the Laboratory for Developmental Research of Advanced Materials, the Institute for Materials Research, Tohoku University.

¹D. B. Rogers, R. D. Shannon, A. W. Sleight, and J. L. Gillson, *Inorg. Chem.* **8**, 841 (1969).

²A. Tanaka, *J. Electron Microsc.* **43**, 177 (1994).

³Y. Hayakawa, K. Fukuzaki, S. Kohiki, Y. Shibata, T. Matsuo, K. Wagatusma, and M. Oku, *Thin Solid Films* (to be published).

⁴Y. Hayakawa, S. Kohiki, and F. Shoji (unpublished).

⁵K. Nishihagi (private communication).

⁶D. D. Sarma and C. N. R. Rao, *J. Electron Spectrosc. Relat. Phenom.* **20**, 25 (1980).

⁷O. K. Andersen, *Phys. Rev. B* **12**, 3060 (1975).

⁸For a review, R. O. Jones and O. Gunnarsson, *Rev. Mod. Phys.* **61**, 689 (1989).

⁹G. Thiele and P. Woditsch, *J. Less-Common Met.* **17**, 459 (1969).

¹⁰L. F. Mattheiss, *Phys. Rev. B* **13**, 2433 (1976).

¹¹J. J. Yeh and I. Lindau, *At. Data Nucl. Data Tables* **32**, 1 (1985).

¹²U. Mizutani, *Phys. Status Solidi B* **176**, 9 (1993).

¹³J. Hafner, *J. Non-Cryst. Solids* **69**, 325 (1985).

¹⁴L. J. van der Pauw, *Philips Res. Rep.* **13**, 1 (1958).